Available online at www.sciencedirect.com
SCIENCE DIRECT®
Energy Conversion and Management 47 (2006) 1159–1178
ENERGY CONVERSION & MANAGEMENT
www.elsevier.com/locate/enconman

Neural network based solar cell model

Engin Karatepe *, Mutlu Boztepe, Metin Colak

Department of Electrical and Electronics Engineering, Faculty of Engineering, Ege University, Bornova, Izmir 35100, Turkey

Received 6 December 2004; received in revised form 28 June 2005; accepted 28 July 2005
Available online 22 September 2005

Abstract

This paper presents a neural network based approach for improving the accuracy of the electrical equivalent circuit of a photovoltaic module. The equivalent circuit parameters of a PV module mainly depend on solar irradiation and temperature. The dependence on environmental factors of the circuit parameters is investigated by using a set of current–voltage curves. It is shown that the relationship between them is nonlinear and cannot be easily expressed by any analytical equation. Therefore, the neural network is utilized to overcome these difficulties. The neural network is trained once by using some measured current–voltage curves, and the equivalent circuit parameters are estimated by only reading the samples of solar irradiation and temperature very quickly without solving any nonlinear implicit equations that is necessary in conventional methods. To verify the proposed model, an experimental set up is installed. The comparison between the measured values and the proposed model results shows higher accuracy than the conventional model for all operating conditions.

Keywords: Photovoltaic module; Equivalent circuit parameter; Artificial neural network; *I–V* characteristics; Modeling

* Corresponding author. Tel./fax: +90 232 3886024.
E-mail address: engin@bornova.ege.edu.tr (E. Karatepe).

0196-8904/$ - see front matter © 2005 Elsevier Ltd. All rights reserved.
doi:10.1016/j.enconman.2005.07.007

1. Introduction

Different solar cell models have been developed to describe the electrical behaviors of solar cells, but the electrical equivalent circuit is a convenient and common way in most simulation studies. The five parameters of interest in the equivalent circuit are the photo-current (I_{ph}), series resistance (R_s), parallel resistance (R_p), diode saturation current (I_s) and the ideality factor (n). The current–voltage (I–V) relationship of a solar cell is described by a mathematical equation that is both implicit and nonlinear. Therefore, determination of the parameters requires more computational efforts for each operating condition [1–7]. While some authors use numerical analysis methods to solve the implicit nonlinear equation of the I–V relation, others use analytical methods with a series of simplifications and approximations. In most studies, only the photo-current and the diode saturation current are changed with irradiation and temperature, respectively. However, all of the circuit parameters depend on both irradiation and cell temperature. Every assumption forces the model to fall into error. For this reason, an assumption should be done carefully, especially under low irradiation conditions and in simulation studies of a partially shaded photovoltaic (PV) array. In this study, the dependence of all the circuit parameters on cell temperature and irradiance are included by using the neural network for improving the accuracy of the PV module model.

In Refs. [2,3], some equations that take into account the effects of changes in irradiance and temperature are proposed for the circuit parameters, and then, these equations are put into the I–V equation of the PV module. This increases the computational effort. In addition, some differences can be seen in the equations that describe the relationship between the parameters and the operational conditions. So, there may still remain uncertainties about some relevant system dynamics after derivation of the model. Blas et al. [4] present the use of analytical methods in determining the circuit parameters for the operation of a solar cell under conditions of high irradiance. Teng and Ping [1] present the determination of the circuit parameters from experimental data by using the Q–R decomposition technique based on the least square method. In addition to such approaches, a number of neural network systems have been developed to model the PV modules in tracking the maximum power point for PV systems [8–10].

An artificial neural network (ANN) is accepted as a technology offering an alternative way to solve complex problems. In the last decade, significant progresses have been made in neural network technology to expand the range of potential applications into different areas because of the black box functionality of neural networks. Also, because of parallel computation techniques, a large number of descriptive features can be used. Photovoltaic module equivalent circuit parameters change with respect to the incident solar irradiation on the PV modules and the temperature of the solar cells. The relationship between them is nonlinear and cannot be easily expressed by an analytical equation. This study uses the advantages of neural networks such as no required knowledge of internal system parameters, less computational effort and a compact solution for multivariable problems. The neural network can provide very good mapping if trained correctly. This makes it a good choice for such a task. The neural network is utilized to predict the equivalent circuit parameters by only reading the samples of irradiation and temperature. A number of available experimental data are used for training the neural network, which employs a backpropagation algorithm.

The main object of this paper is to investigate the applicability of the neural network based PV equivalent circuit model for improving the model accuracy and to show the necessity of including the variation of all the parameters with varying operating conditions.

From here on, the paper is organized as follows. In the second part, the conventional equivalent circuit of a solar cell model is reviewed. In the third, variations of the PV equivalent circuit parameters under different operating conditions are investigated. In the fourth, the structure of the neural network, the training procedures and testing are explained. In the fifth, the proposed model with the data available from the experimental set up is presented. In the last part, the results and some concluding remarks are given.

2. Conventional electrical circuit of a PV model

A photovoltaic module is the basic element of each photovoltaic system. It consists of many jointly connected solar cells. A number of solar cell models have been developed [5,11–16], but the one diode electrical equivalent circuit is commonly used for cell based or module based analysis. It is given in Fig. 1. The one diode equivalent circuit of a solar cell consists of a diode, a current source, a series resistance and a parallel resistance. The current source generates the photo-current (I_{ph}) that is a function of the incident solar irradiation and cell temperature. The diode represents the p–n junction of a solar cell. The temperature dependence of the diode saturation current (I_s) and constant diode ideality factor (n) are included in the modeling. At real solar cells, a voltage loss on the way to the external contacts is observed. This voltage loss is expressed by a series resistance (R_s). Furthermore leakage currents are described by a parallel resistance (R_p). Using Kirchhoff's first law, the equation for the extended I–V curve is derived as follows:

$$I = I_{ph} - I_s\left\{\exp\left[\frac{q(V + IR_s)}{nN_skT}\right] - 1\right\} - \frac{V + IR_s}{R_p} \tag{1}$$

where I is the output current of the PV module, N_s is the number of solar cells in series in a module, V is the terminal voltage of the module, q is the electric charge (1.6×10^{-19} C), k is the Boltzmann constant (1.38×10^{-23} J/K) and T is the cell temperature (K).

In the conventional approach, to decrease the complexity, it is assumed that only the photocurrent and the diode saturation current depend on the operational conditions. These dependencies are included by using Townsend equations [15] that are given as follows:

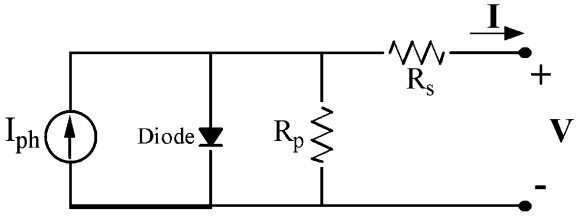

Fig. 1. PV module equivalent circuit.

$$I_{\mathrm{ph}} = \frac{G}{G_{\mathrm{ref}}}\left[I_{\mathrm{ph,ref}} + \mu_{I_{\mathrm{SC}}}(T - T_{\mathrm{ref}})\right] \tag{2}$$

$$I_{\mathrm{s}} = I_{\mathrm{s,ref}}\left(\frac{T}{T_{\mathrm{ref}}}\right)^{3} \exp\left[\frac{qE_{\mathrm{g}}N_{\mathrm{s}}}{kn}\left(\frac{1}{T} - \frac{1}{T_{\mathrm{ref}}}\right)\right] \tag{3}$$

where G is the incident solar irradiation on the PV module, E_{g} is the material bandgap energy of the solar cell material, $\mu_{I_{\mathrm{SC}}}$ is the temperature coefficient of the short circuit current. The subscript ref denotes the value of the related parameter at the reference operating condition. The series resistance, parallel resistance and diode ideality factor are usually determined once for a reference operating condition, and then, these values are also used for other conditions. The parallel resistance usually is assumed large enough to be accurately approximated as infinite [11,15,17].

3. Variation of one diode model parameters

To characterize a PV module as a power source in studying its performance, it is very important to take into consideration the dependence of all the equivalent circuit parameters of the PV module on irradiation and cell temperature. The five equivalent circuit parameters can be determined using the available operating points on the I–V curve of the module. To be able to obtain the changes of the parameters over the whole range of operating conditions, Sandia's PV module electrical performance model [18] is used for generating the required five points on the I–V curve. These points are shown in Fig. 2 for one operating condition. These points are generated for 209 operating conditions between 15–65 °C and 100–1000 W/m^2 to solve the five coupled implicit nonlinear equations for the Siemens SM-55 PV module that consists of 36 series connected monocrystalline silicon solar cells. Solving the nonlinear implicit system of equations involves finding a

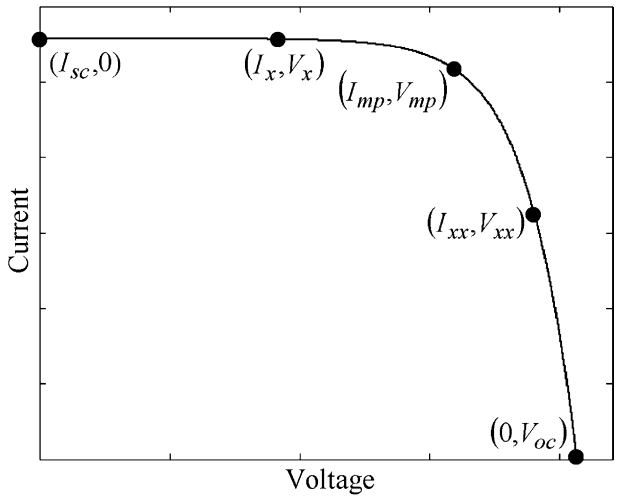

Fig. 2. The used five operating points on the I–V curve of PV module to solve the nonlinear implicit I–V equation for a single operating condition.

solution such that every equation in the nonlinear system is 0. That is, we have five equations and five unknowns for each operating condition and we want to find $x \in \Re^5$ such that $F(x) = 0$, where

$$F_i = -I_i + x_1 - x_2(\exp(q(V_i + I_i x_4)/x_3 N_s kT) - 1) + (V_i + I_i x_4)/x_5 \tag{4}$$

$$F(x) = \begin{bmatrix} F_1(x) \\ F_2(x) \\ F_3(x) \\ F_4(x) \\ F_5(x) \end{bmatrix} \tag{5}$$

Different optimization methods are tried for solving the system of equations. Numerical exercises seem to indicate that the trust region method [19] is considerably better than the others, so this method is used. In general, trust region methods are faster than gradient methods and guarantee stability regardless of the initial conditions. Good initial values are important for solving nonlinear system equations. An initial value that satisfies or closely satisfies many of the constraints reduces the work involved in finding a first feasible solution. At each different operating condition, initial values of the photo-current, series resistance and parallel resistance are estimated from their corresponding I–V curves. Initial values of the parameters are denoted by the subscript 0 and are given as

$$I_{ph0} = I_{sc} \tag{6}$$

$$R_{s0} = (V_{oc} - V_{xx})/I_{xx} \tag{7}$$

$$R_{p0} = V_x/(I_{sc} - I_x) \tag{8}$$

where I_{sc} is the short circuit current, I_x is the current at $V_x = 0.5V_{oc}$, I_{xx} is the current at $V_{xx} = 0.5(V_{oc} + V_{mp})$, V_{oc} is the open circuit voltage and V_{mp} is the voltage at the maximum power point. The initial value of the diode ideality factor is taken as 1.5 for all cases. An initial value of the diode saturation current is determined by using Eq. (3).

The solution of the system equations showed that all the parameters depend on both irradiation and temperature. As shown in Figs. 3–7, it is difficult to give a clear functional relationship. On the other hand, it is necessary to include the variation of the parameters properly if accurate and reliable performance estimation is required in simulation studies. Obviously, it is quite difficult to determine the parameters for each irradiation and temperature in running simulation studies or on line PV system applications. For this reason, all parameters are estimated by using the neural network.

4. ANN based parameters prediction

The artificial neural network structure is one of the important factors that influence the learning performances of networks. It is a natural hope to employ as small structures as possible under the conditions that they meet the performance requirements. Experience has shown that using the smallest network that can learn the task is better for both practical and theoretical reasons.

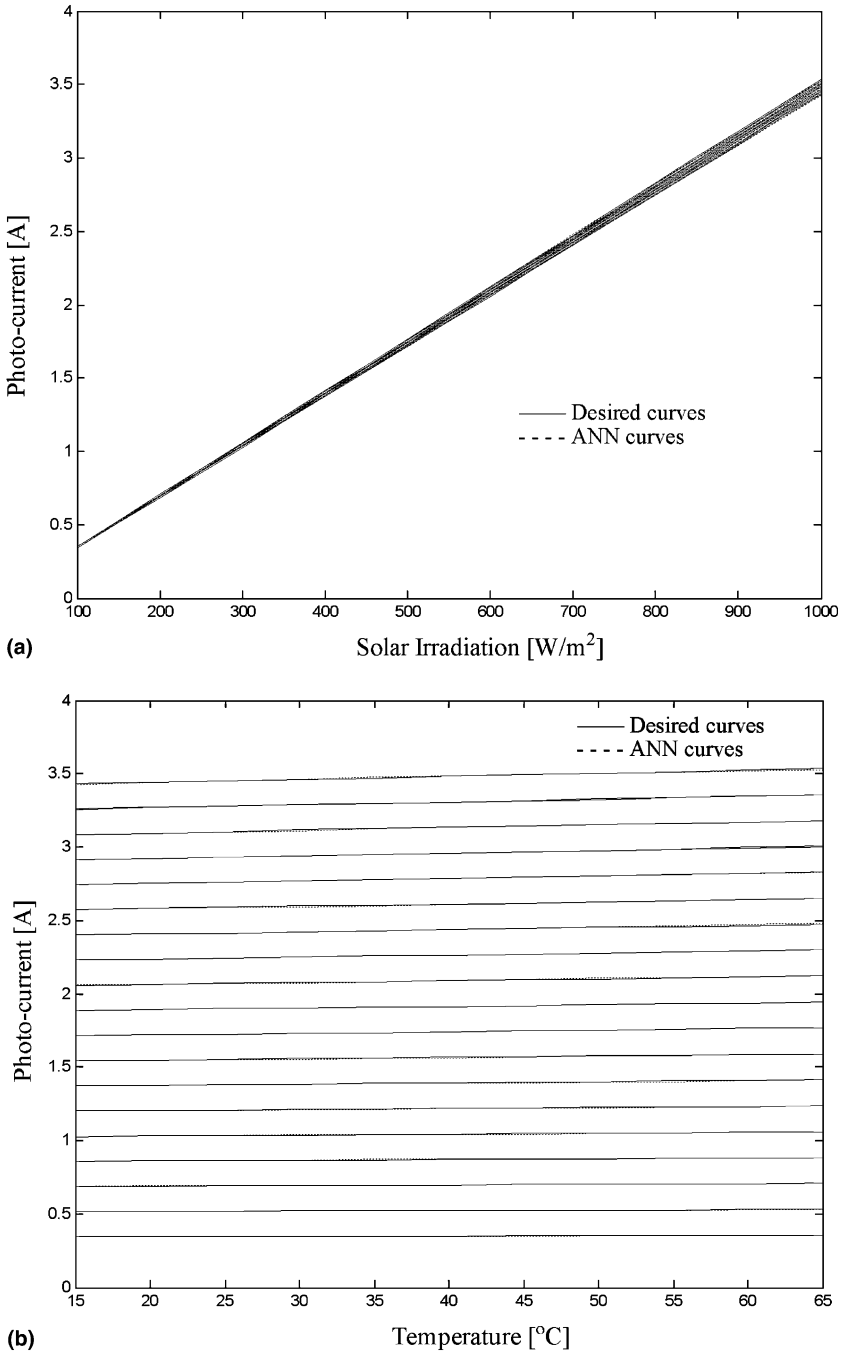

Fig. 3. Variation of the photo-current with (a) irradiance, (b) temperature and the comparison of desired values (solid line) with the ANN predicted (dashed line) values (which are indistinguishable from desired values).

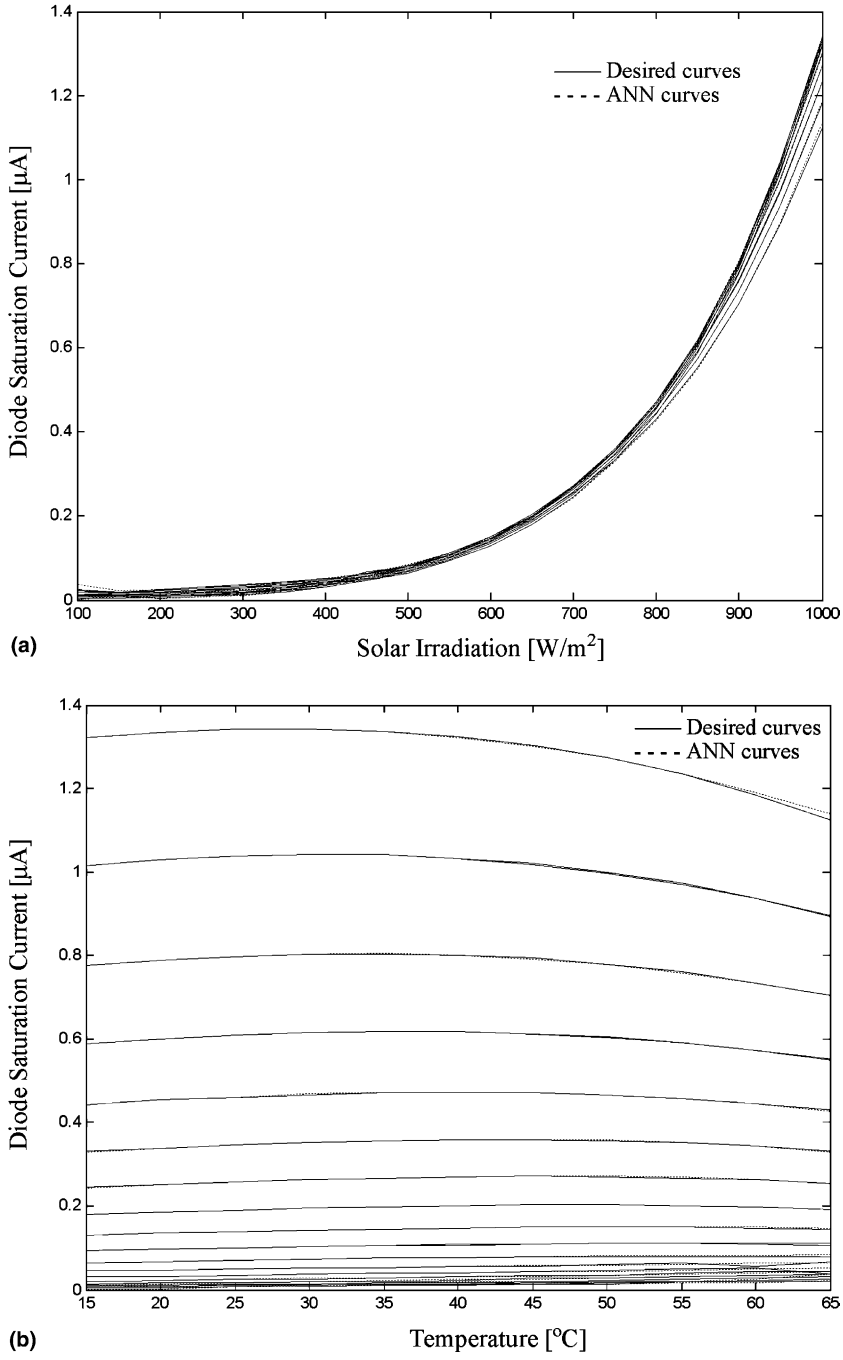

Fig. 4. Variation of the diode saturation current with (a) irradiance, (b) temperature and the comparison of desired values (solid line) with the ANN predicted (dashed line) values.

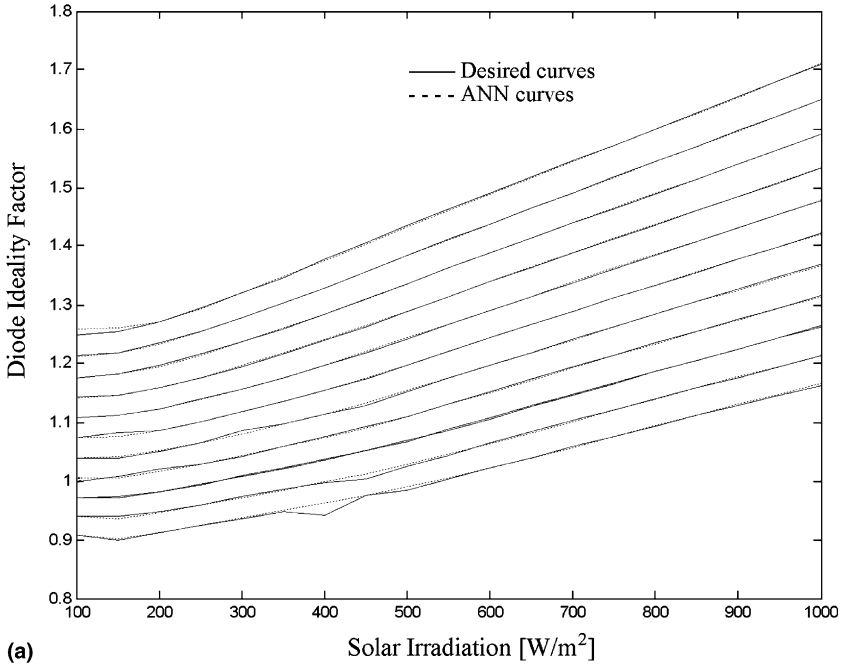

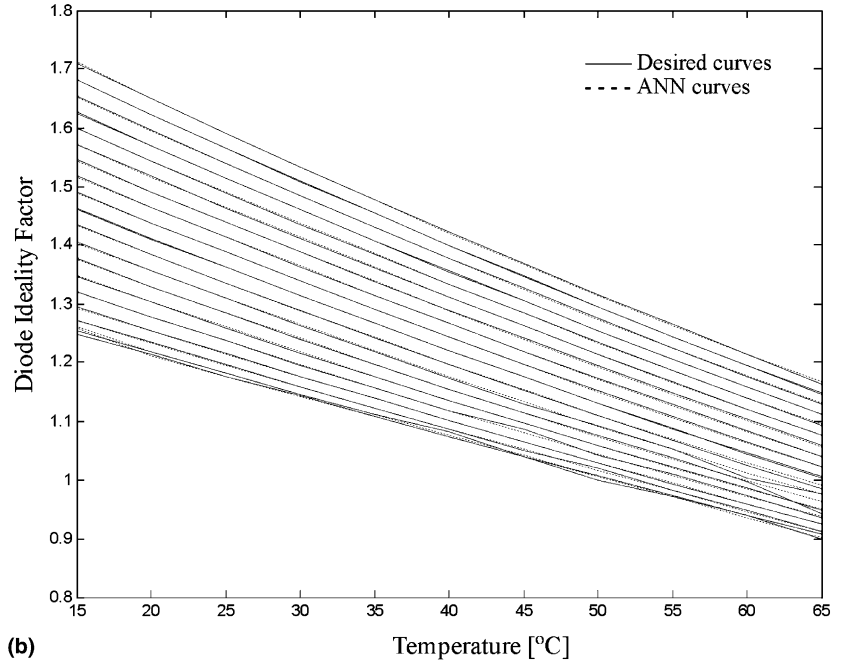

Fig. 5. Variation of the diode ideality factor with (a) irradiance, (b) temperature and the comparison of desired values (solid line) with the ANN predicted (dashed line) values.

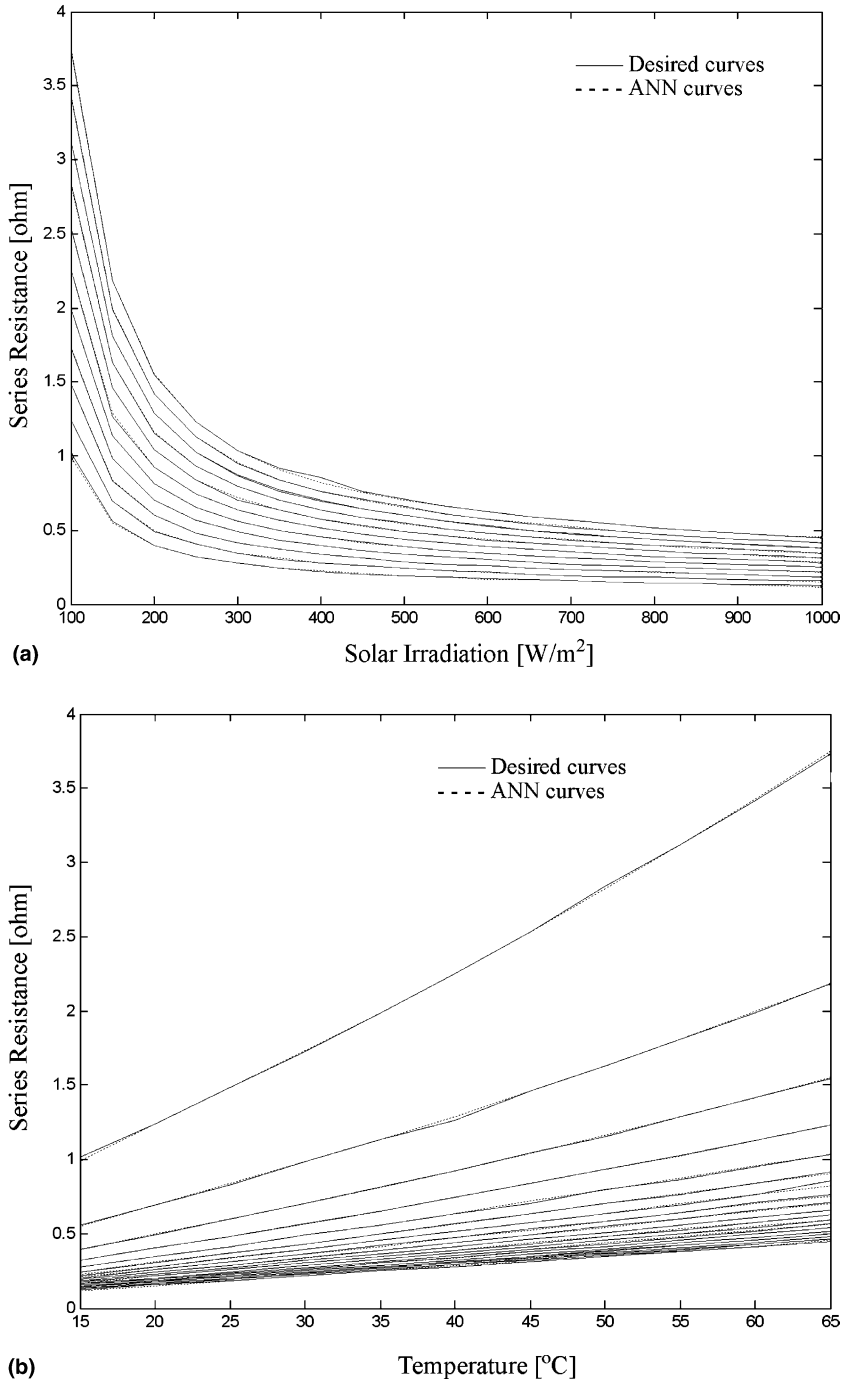

Fig. 6. Variation of the series resistance with (a) irradiance, (b) temperature and the comparison of desired values (solid line) with the ANN predicted (dashed line) values.

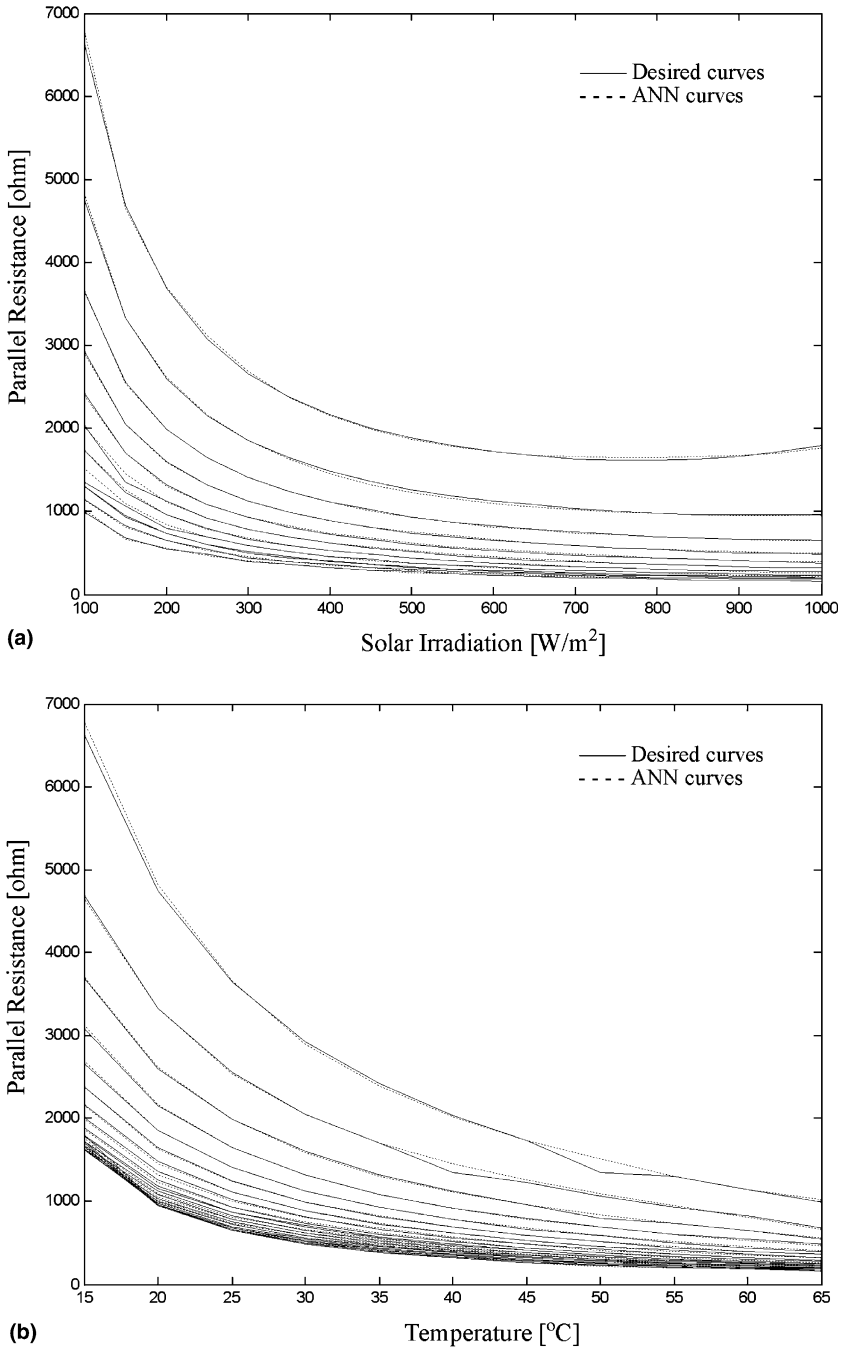

Fig. 7. Variation of the parallel resistance with (a) irradiance, (b) temperature and the comparison of desired values (solid line) with the ANN predicted (dashed line) values.

Training a smaller network usually requires less computation because each iteration is computationally less expensive. Unfortunately, the structures of multilayer feedforward perceptron networks are mainly determined by experience, and there has not been found a valid formula that is suitable for the different situations [20–23]. Architecture selection of ANN techniques can be divided into two categories. In the first category, a big network is selected, and the unnecessary nodes or connections are gradually eliminated [20]. The second category begins with a small network and gradually adds nodes or connections as needed. In this study, to map the relationship between n, I_s, R_s, R_p, I_{ph} and the irradiation and cell temperature, the second category was used when an appropriate neural network size is selected. Finally, sufficient results were obtained for a three layer feedforward neural network (input, single hidden and output layers) as shown in Fig. 8.

The number of nodes in the input and the output layers are based on the input and output dimensions, respectively. The number of hidden layer nodes is determined empirically as we stated above. The 20 hidden nodes gave the most accurate estimation, and therefore, only the results of this case are given in the paper. Consequently, the input layer has 2 nodes, the hidden layer has 20 nodes and the output layer has 5 nodes (see Fig. 8). The input layer in this case consists of a two dimensional vector, irradiation and temperature, and the output vector is a five dimensional vector comprising n, I_s, R_s, R_p and I_{ph}. To reduce the computational effort, we take into consideration a small size network when we find an appropriate network size. This is very important during the testing phase of the network where fast responses are usually required.

The outputs of the input layer nodes are weighted, summed, and passed through an activation function that acts as an amplitude limiting function. Three basic types of activation functions exist: threshold functions, piece wise linear function and sigmoid function [22]. The activation functions are used to limit or squash the input to the next neuron layer. The learning signal is a

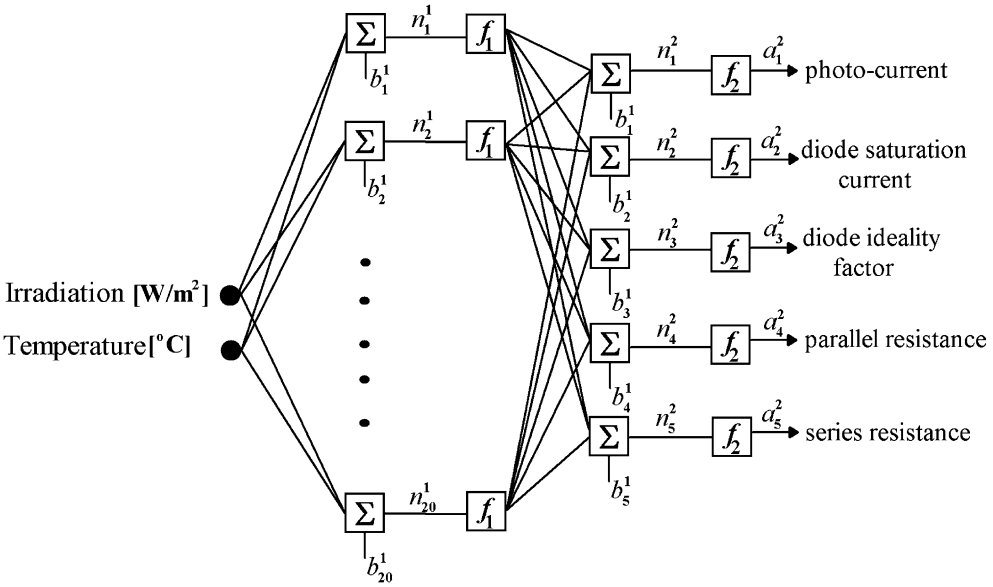

Fig. 8. Configuration of artificial neural network.

function of the error multiplied by the gradient of the activation function. For training, the activation function must be monotonically increasing from left to right, differentiable and smooth. In this study, all data are scaled to the range $\{-1;1\}$, and a hyperbolic tangent sigmoid transfer function is used as the activation function of the single hidden layer [24]. A pure linear function was used as the activation function of the output layers of the neural network of Fig. 8, similar to Ref. [25]. Using a linear function in the output node of the neural network reduces the resulting computations [9]. The relations between the inputs and outputs are given as follows:

The input vector $x = [\text{irradiation}, \text{cell temperature}]$ is applied to the input layer of the network as shown in Fig. 8. The net input of the jth hidden unit is

$$n_j^1 = \sum_{i=1}^{2} w_{ji} x_i + b_j^1 \tag{9}$$

where w_{ji} is the weight on the connection from the ith input unit, b_j^h for $j = 1, 2, \ldots, 20$ represent the bias for the hidden layer neurons. The output of the neurons in the hidden layer is

$$a_j^1 = f_1\left(\sum_{i=1}^{2} w_{ji} x_i + b_j^1\right) \tag{10}$$

$$f_1(n) = \text{tansig}(n) = \frac{2}{1 - e^{-2n}} - 1 \tag{11}$$

and the net input to the neurons in the output layer is written as

$$n_k^2 = \sum_{j=1}^{20} w_{kj} a_j^1 + b_k^2 \tag{12}$$

where w_{kj} is the weight on the connection from the jth input unit, b_k^2 for $k = 1, 2, \ldots, 5$ represent the bias for the second layer neurons. The output of the second layer, a_k^2, is the network outputs of interest, and these outputs are labeled y_k.

$$a_k^2 = y_k = f_2\left(\sum_{j=1}^{20} w_{kj} a_j^1 + b_k^2\right) \tag{13}$$

$$f_2(n) = \text{purelin}(n) = n \tag{14}$$

The learning stage of the network is performed by updating the weights and biases using a backpropagation algorithm with the Levenberg-Marquardt optimization method (see e.g. [26]) in order to minimize the sum of squared differences between the network targets and actual outputs for a given input vector. In order to avoid the network losing its generalization ability, training was stopped when the error on the test set was beginning to rise considerably (roughly after about 1000 training epochs). Fig. 9 shows the objective function (the sum squared error) evolution for the first 250 training iterations. The prediction of the ANN is also plotted in Figs. 3–7. Each curve represents an operating condition. As can be seen clearly, the ANN can be used to identify the PV model parameters excellently.

The basic configuration of the proposed PV model is summarized in Fig. 10. It is composed of a two stage process. Firstly, a neural network is used to predict the five parameters by reading only

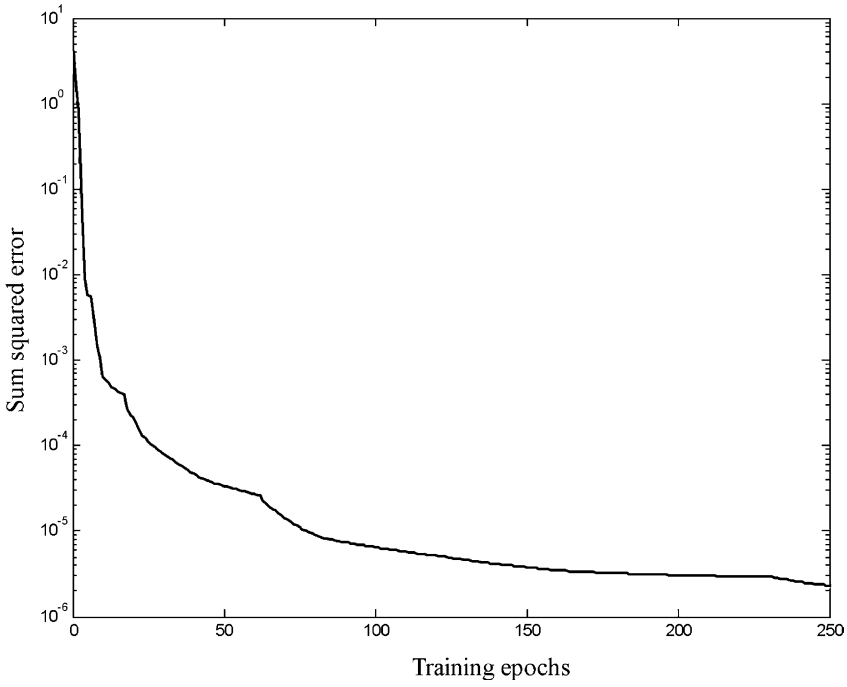

Fig. 9. Representation of the error trend as obtained with the first 250 iterations of the training algorithm of ANN.

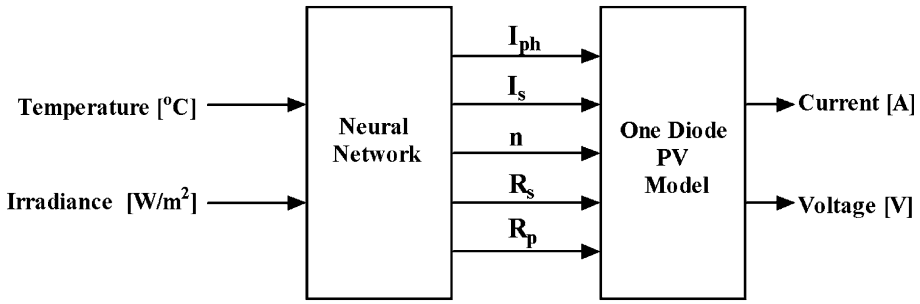

Fig. 10. The basic configuration of the proposed PV model.

the samples of irradiation and temperature. Secondly, these parameters are put into the one diode electrical equivalent circuit model.

5. Application of the proposed model on experimental data

In order to investigate the efficiency of the proposed neural network based model, two distinct tests were performed. The first test includes data that was obtained from Sandia National Laboratory's (SNL) PV module electrical performance model [18] for the SM-55 PV module. The

Table 1
Specification of SM-55 and OST-80 PV module

	SM-55 PV module	OST-80 PV module
Maximum power (P_{mp}) (W)	55	80
Open circuit voltage (V_{oc}) (V)	21.7	22
Short circuit current (I_{sc}) (A)	3.45	4.90
Operating voltage at maximum power (V_{mp}) (V)	17.4	18
Operating current at maximum power (I_{mp}) (A)	3.15	4.50

AM 1.5, 1000 W/m^2, 25 °C.

second test includes data that was obtained from outdoor measurements by installing an experimental set up for the OST-80 PV module, composed of polycrystalline silicon solar cells and manufactured by Orjin Solar Technology Ltd. in Turkey. Table 1 shows the specifications of the SM-55 and OST-80 PV modules.

5.1. Model testing using SNL's PV model for SM-55 PV module

Sandia National Laboratories have developed the model to predict the electrical output of photovoltaic modules [18,27,28]. The performance of the SNL model is empirically based, and the individual equations used in the SNL model are derived from individual solar cell characteristics. Sandia builds detailed outdoor performance tests on commercially available modules, and a database of the associated module performance parameters is maintained on the Sandia website (http://www.sandia.gov/pv). These module parameters were used directly in the performance model for the SM-55 PV module in this study, as we mentioned earlier.

The required five operating points for the proposed model (see Fig. 2) were obtained by using the SNL's latest implementation of the model [18]. The three classic points on the module I–V curve (short circuit point, open circuit point and maximum power point) and two additional points (a point at a voltage equal to one half of the open circuit voltage and a point at a voltage midway between maximum power voltage and open circuit voltage) are given in Ref. [18]. Neural network training data should be selected to cover the entire region where the network is expected to operate. The generated data set for 209 operating conditions between 15–65 °C and 100–1000 W/m^2 in Section 4 was subdivided into a training set (191 sets) that well describes the entire problem domain and a test set (18 sets), which are given in Tables 2 and 3. The neural network generated values are applied to the equivalent circuit model (see Fig. 10).

In the conventional model described in Section 2, Eq. (2) gives the light generated current I_{ph} as a function of irradiance G [W/m^2] and $I_{ph,ref}$ is the module's short circuit current at reference irradiance G_{ref} (650 W/m^2), the temperature coefficient for the current of the SM-55 PV module $\mu_{I_{sc}}$ is 5.5×10^{-4}. This reference irradiance gave the most accurate performance for both low irradiation and high irradiation levels. In general, most studies use 1000 W/m^2 as the reference irradiance because it is easily available from catalog information. This forces the model to fall into error, especially at low irradiation levels. Eq. (3) accounts for the temperature dependency of the reverse saturation current I_s that is a function of the reference reverse saturation current $I_{s,ref}$ at the reference temperature T_{ref} (25 °C). The series resistance of the module and the ideality factor can be

Table 2
The current, voltage and power values at maximum power point of the SM-55 PV module for testing data

Operating condition		SNL model values			Conventional model			The proposed model		
G [W/m^2]	T [°C]	V_{mp} [V]	I_{mp} [A]	P_{mp} [W]	V_{mp} [V]	I_{mp} [A]	P_{mp} [W]	V_{mp} [V]	I_{mp} [A]	P_{mp} [W]
150	25	16.381	0.480	7.871	15.336	0.470	7.220	16.375	0.478	7.841
250		16.822	0.799	13.446	16.050	0.787	12.634	16.799	0.799	13.430
350		17.046	1.116	19.038	16.491	1.105	18.236	17.029	1.117	19.032
450		17.178	1.433	24.618	16.843	1.423	23.968	17.187	1.432	24.618
550		17.262	1.748	30.176	17.107	1.741	29.798	17.251	1.749	30.176
650		17.318	2.061	35.706	17.320	2.061	35.706	17.337	2.059	35.706
750		17.355	2.374	41.206	17.514	2.379	41.680	17.351	2.374	41.206
850		17.379	2.685	46.672	17.695	2.696	47.707	17.402	2.682	46.672
950		17.394	2.995	52.106	17.838	3.014	53.782	17.388	2.996	52.106
150	45	14.472	0.479	6.943	13.673	0.467	6.388	14.484	0.476	6.900
250		14.971	0.798	11.947	14.402	0.783	11.284	14.971	0.795	11.916
350		15.224	1.115	16.975	14.886	1.100	16.382	15.218	1.114	16.958
450		15.372	1.430	21.995	15.260	1.416	21.618	15.390	1.429	21.995
550		15.467	1.745	26.995	15.525	1.736	26.960	15.470	1.744	26.995
650		15.529	2.058	31.967	15.762	2.054	32.387	15.520	2.059	31.967
750		15.570	2.370	36.910	15.957	2.374	37.882	15.548	2.373	36.909
850		15.597	2.681	41.820	16.137	2.691	43.437	15.606	2.679	41.820
950		15.614	2.990	46.698	16.282	3.012	49.042	15.604	2.992	46.698

determined by using Eq. (1), and the values were found as 0.052 and 1.65 Ω, respectively. As can be shown in Tables 2 and 3, the proposed model generates satisfactory results for all operating conditions.

5.2. Model testing using outdoor measurement for OST-80 PV module

The PV module and measuring apparatus were installed on the rooftop of the Electrical–Electronics Engineering building of the campus of Ege University. The OST-80 PV module is composed of 36 polycrystalline silicon solar cells. The current–voltage characteristics of the PV module as well as the corresponding module temperature and solar irradiance were acquired by using the personal computer based data acquisition system (DAS). The DAS interface uses a 10 bit A/D converter and includes an electronic load, a weather station and a computer controlled I–V curve tracer. The module back surface temperature was measured by using a Type-T thermocouple at the center of the back of the PV module with a temperature sensor accuracy ±1.0 °C in a range from −40 to +350 °C. The solar irradiance was measured with a Kipp & Zonen CM-3 pyranometer [29,30] installed at the same azimuth and tilt angle as the PV module. It is a thermopile pyranometer with flat spectral response from 305 to 2800 nm. The irradiance variation was achieved by triggering the I–V curve sweep at different times during the day of the light. The range of temperature was obtained as follows. First of all, we covered the front side of the module completely and waited until thermal equilibrium was reached. After that, the module was quickly uncovered and I–V curve data were recorded consecutively until the module temperature reached the normal operating module temperature.

Table 3
Percentage errors of the current, voltage and power values at maximum power point of the SM-55 PV module for testing data

Operating condition		Conventional model			The proposed model		
G [W/m^2]	T [°C]	V_{mp} [%]	I_{mp} [%]	P_{mp} [%]	V_{mp} [%]	I_{mp} [%]	P_{mp} [%]
150	25	6.379	2.083	8.271	0.037	0.417	0.381
250		4.589	1.502	6.039	0.137	0.000	0.119
350		3.256	0.986	4.213	0.100	0.090	0.032
450		1.950	0.698	2.640	0.052	0.070	0.000
550		0.898	0.400	1.253	0.064	0.057	0.000
650		0.012	0.049	0.020	0.110	0.097	0.000
750		0.916	0.211	1.150	0.023	0.000	0.000
850		1.818	0.410	2.218	0.132	0.112	0.000
950		2.553	0.634	3.217	0.034	0.033	0.000
150	45	5.521	2.505	7.994	0.083	0.626	0.619
250		3.801	1.880	5.550	0.000	0.376	0.259
350		2.220	1.345	3.493	0.039	0.090	0.100
450		0.729	0.979	1.714	0.117	0.070	0.000
550		0.375	0.516	0.130	0.019	0.057	0.000
650		1.500	0.194	1.314	0.058	0.049	0.000
750		2.486	0.169	2.633	0.141	0.127	0.003
850		3.462	0.373	3.867	0.058	0.075	0.000
950		4.278	0.736	5.019	0.064	0.067	0.000

The module I–V curves were obtained with several irradiations ranging from 42 to 856 W/m^2 and cell temperatures from 27 to 47 °C. As we stated earlier, the required five operating points are selected from measured I–V curves as shown in Fig. 2 with corresponding module temperature and irradiance.

In this study, the neural network (see Fig. 8) was trained to identify the equivalent circuit parameters from 49 different I–V curves. The eight of them (see Table 4) that have no part in the training data are presented to the neural network to test its generalization. Generalization

Table 4
The current, voltage and power values at maximum power point of the OST-80 PV module for testing data

Operating condition		Measured			Conventional model			The proposed model		
G [W/m^2]	T [°C]	V_{mp} [V]	I_{mp} [A]	P_{mp} [W]	V_{mp} [V]	I_{mp} [A]	P_{mp} [W]	V_{mp} [V]	I_{mp} [A]	P_{mp} [W]
851.84	46.65	15.003	3.734	56.021	15.559	3.734	58.103	14.816	3.701	54.837
712.24	45.82	14.637	3.187	46.648	15.381	3.119	47.985	14.880	3.095	46.068
568.57	28.77	16.780	2.463	41.329	16.438	2.520	41.439	16.579	2.497	41.397
496.73	43.63	15.595	2.111	32.921	15.057	2.171	32.690	15.304	2.158	33.029
321.23	42.70	14.806	1.457	21.572	14.466	1.401	20.270	14.905	1.447	21.574
153.67	40.93	15.285	0.547	8.360	13.508	0.635	8.557	14.817	0.565	8.380
81.84	44.98	14.637	0.323	4.727	12.166	0.349	4.252	14.223	0.330	4.700
43.84	30.96	14.552	0.166	2.415	12.456	0.189	2.354	14.447	0.167	2.415

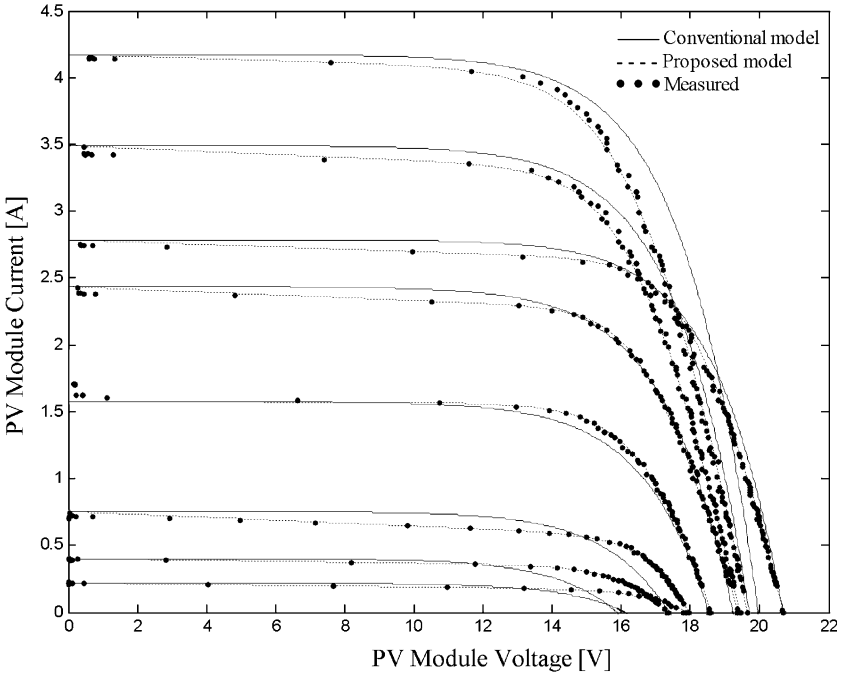

Fig. 11. The comparison of conventional model and the proposed model for testing data set with measured I–V curves of the OST-80 PV module.

is defined as the ability of the neural network to map correctly new points that have not taken part in the training. We have observed that there is enough information in this training data to perform the desired mapping.

For the conventional model, the reference irradiance and reference temperature were taken as 500 W/m^2 and 29 °C, respectively. The temperature coefficient for the current of the OST-80 PV module $\mu_{I_{sc}}$ is 2.39×10^{-4}. The series resistance and diode ideality factor are determined as 0.106 and 1.8 Ω, respectively.

Figs. 11 and 12 shows the current–voltage and power–voltage characteristic curves for the testing data. As can be seen clearly, the curves from the proposed model are better than those of the conventional model in fitting the measured values under all the conditions.

6. Results and discussion

The current, voltage and power values at the maximum power point were determined for the testing data and are presented in Tables 2–5. Better results for the current, voltage and power are observed with the proposed model. The conventional model causes relatively large error, especially under low irradiation conditions, so such model can reduce the accuracy of simulation results in finding the overall I–V curve of series/parallel connected solar cells that have nonidentical I–V characteristics. The I–V characteristics of series interconnected solar cells can be found

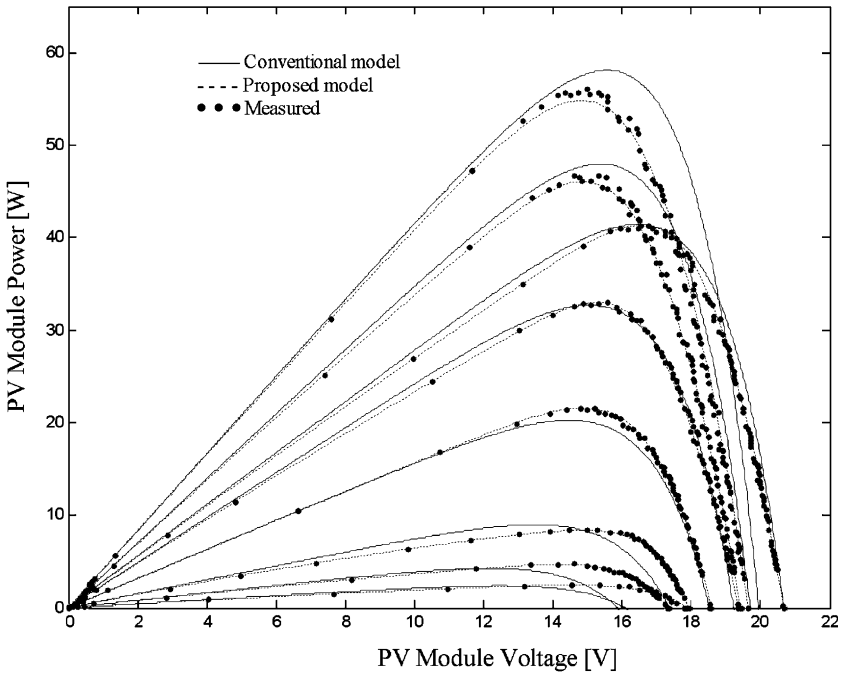

Fig. 12. The comparison of conventional model and the proposed model for testing data set for the power–voltage curves of the OST-80 PV module.

Table 5
Percentage errors of the current, voltage and power values at maximum power point of the OST-80 PV module for testing data

Operating condition		Conventional model			The proposed model		
G [W/m^2]	T [°C]	V_{mp} [%]	I_{mp} [%]	P_{mp} [%]	V_{mp} [%]	I_{mp} [%]	P_{mp} [%]
851.84	46.65	3.709	0.000	3.717	1.245	0.877	2.112
712.24	45.82	5.085	2.111	2.867	1.665	2.860	1.242
568.57	28.77	2.036	2.350	0.266	1.196	1.379	0.166
496.73	43.63	3.449	2.847	0.700	1.862	2.234	0.330
321.23	42.70	2.295	3.829	6.035	0.671	0.656	0.011
153.67	40.93	11.622	16.087	2.356	3.058	3.392	0.240
81.84	44.98	16.876	8.211	10.036	2.822	2.315	0.556
43.84	30.96	14.397	13.866	2.501	0.716	0.722	0.000

by adding the individual voltages for each current. On the other hand, for parallel solar cells, the currents of the individual solar cells must be added at each voltage. Therefore, accurate prediction of the solar cell model is very important when electrical mismatch losses are analyzed. The main cause of mismatching between solar cells is partial shadowing. The parallel resistance, representing the leakage current, and the series resistance values are effective parameters when the PV module is partially shaded [31,32]. As can also be seen in Figs. 6 and 7(a), the changes of the parallel and series resistances become more effective when the irradiation levels are lower than 500 W/m^2.

So, the equivalent circuit parameters of the PV module must be determined for all operating conditions.

These results show that the proposed model for a solar cell model significantly decreases the error in simulation studies and also offers a compact solution to include the dependence of the equivalent circuit parameters on solar irradiation and cell temperature.

7. Conclusions

The paper describes an application of artificial neural networks to PV module modeling. The accuracy and generalization of the proposed model is demonstrated by comparing test results with actual data. In the conventional PV model, the dependency on solar irradiation and cell temperature of all the model parameters are not included, so the accuracy and the reliability of performance estimation cannot be sufficient for all operating conditions. This paper accepts irradiance and temperature as variable parameters for all the parameters of the PV module equivalent circuit model. They are predicted by reading only samples of radiation and temperature by using an artificial neural network. After that, these parameters are presented to the current–voltage equation of the PV module to obtain the electrical characteristics. The trained network is sufficiently accurate in representing the variation of the parameters when compared with other methods. The proposed model can be used for any type of PV module and on line applications in power electronics studies.

Acknowledgements

The authors wish to acknowledge financial support provided by the Ege University Research Fund, Orjin Solar Technology Inc., Izmir, Turkey, and the Solar Energy Institute in Ege University. In addition, the valuable comments of the reviewers are gratefully acknowledged.

References

[1] Teng KF, Ping W. PV module characterization using *Q–R* decomposition based on the least square method. IEEE Trans Indust Electron 1989;36(1):71–5.
[2] Lin L, Yang HX. A study on simulations of the power output and practical models for building systems. J Solar Energy Eng 2004;126:929–35.
[3] Gow JA, Manning CD. Development of photovoltaic array model for use in power-electronics simulation studies. IEE Proc Electron Power Appl 1999;146(2):193–200.
[4] Blas MA, Torres JL, Prieto E, Garcia A. Selecting a suitable model for characterizing photovoltaic devices. Renew Energy 2002;25:371–80.
[5] Kenji A, Masafumi Y. Novel equivalent circuit model and statistical analysis in parameters identification. Solar Energy Mater Solar Cells 2003;75:457–66.
[6] Merten J, Asensi JM, Voz C, Shah AV, Platz R, Andreu J. Improved equivalent circuit and analytical model for amorphous silicon solar cells and modules. IEEE Trans Electron Dev 1998;45(2):423–9.
[7] El-Adawi MK, Al-Nuaim IA. A method to determine the solar cells series resistance from a single *I–V* characteristic curve considering its shunt resistance—new approach. Vacuum 2002;64:33–6.

[8] Al-Amoudi A, Zhang L. Application of radial basis function networks for solar-array modelling and maximum power-point prediction. IEE Proc Gener Transm Distrib 2000;147(5):310–6.
[9] Hiyama T, Kitabayashi K. Neural network based estimation of maximum power generation from PV module using environmental information. IEEE Trans Energy Convers 1997;12(3):241–7.
[10] Veerachary M, Senjyu T, Uezato K. Neural-network-based maximum-power-point tracking of coupled-inductor interleaved-boost-converter-supplied PV system fuzzy controller. IEEE Trans Indust Electron 2003;50(4):749–58.
[11] Walker G. Evaluating MPPT converter topologies using a Matlab PV model. J Electr Electron Eng 2001;21(1):49–56.
[12] Adjakou R, Lishou C, Dieye N, Protin L. Using state-space representation for the monetization of photovoltaic systems. Appl Math Computat 2001;124:129–38.
[13] Hoque A, Wahid A. New mathematical model of a photovoltaic generator. J Electr Eng 2000;28(1).
[14] Shengyi L, Dougal RA. Dynamics multiphysics model for solar array. IEEE Trans Energy Convers 2002;17(2):285–94.
[15] Duffie JA, Beckman WA. Solar engineering and thermal processes. John Wiley & Sons Ltd.; 1991.
[16] Merten J, Asensi JM, Voz C, Shah V, Platz R, Andreu J. Improved equivalent circuit and analytical model for amorphous silicon solar cells and modules. IEEE Trans Electron Dev 1998;45(2):423–9.
[17] Kuo YC, Liang TJ, Chen JF. Novel maximum-power-point-tracking controller for photovoltaic energy conversion system. IEEE Trans Indust Electron 2001;48(3):594–601.
[18] King DL. Sandia's PV module electrical performance model (version, 2000). Sandia National Laboratories; Albuquerque, New Mexico.
[19] McCartin BJ. A model-trust region algorithm utilizing a quadratic interpolate. J Computat Appl Math 1998;91:249–59.
[20] Reed R. Pruning algorithms—a survey. IEEE Trans Neural Networks 1993;4(5):740–7.
[21] Ghosh AK, Lubkeman DL. The classification of power system disturbance waveforms using a neural network approach. IEEE Trans Power Delivery 1995;10(1):109–15.
[22] Zurada JM. Introduction to artificial neural systems. West Publishing Company; 1992.
[23] Curry B, Morgan PH. Model selection in neural networks: some difficulties. Eur J Operat Res 2004, in press, doi:10.1016/j.ejor.2004.05.026.
[24] Kalman B, Kwasny SC. Why Tanh: choosing a sigmoidal function. IEEE Int Joint Conf Neural Network 1992;4:578–81.
[25] Beccali M, Cellura M, Brano VL, Marvuglia A. Forecasting daily urban electric load profiles using artificial neural networks. Energy Convers Manage 2004;45:2879–900.
[26] Scales LE. Introduction to non-linear optimization. New York: Springer-Verlag Inc.; 1985.
[27] King DL, Kratochvil JA, Boyson WE, Bower WI. Field experience with a new performance characterization procedure for photovoltaic arrays. In: 2nd world conference and exhibition on photovoltaic solar energy conversion, 1998.
[28] King DL. Photovoltaic module and array performance characterization methods for all system operating conditions. In: Proceedings of NREL/SNL photovoltaics program review meeting, 1996.
[29] Scofield JH, Cohen PS, Gould S. Real-time, Web based energy monitoring system for a solar academic building. In: Solar 2004 conference proceedings. Portland: 2004.
[30] Togrul IT, Onat E. A study for estimating solar radiation in Elazig using geographical and meteorological data. Energy Convers Manage 1999;40:1577–84.
[31] Sharma AK, Dwivedi R, Srivastava SK. Performance analysis of a solar array under shadow condition. IEE Proc-G 1991;138(3):301–6.
[32] Herrmann W, Wiesner W. Modelling of PV modules—the effects on non-uniform irradiance on performance measurements with solar simulators. In: 16th European photovoltaic solar energy conference, 2000.